Surface-tension-induced flattening of a nearly plane elastic solid

Anand Jagota, Dadhichi Paretkar, and Animangsu Ghatak

Phys. Rev. E **85**, 051602 — Published 11 May 2012

DOI: 10.1103/PhysRevE.85.051602

Surface Tension Induced Flattening of a Nearly Plane Elastic Solid

Anand Jagota[1,2*], Dadhichi Paretkar[1], Animangsu Ghatak[1,3*]

[1]INM-Leibniz Institute for New Materials and Saarland University, Campus D 2 2, 66123 Saarbruecken, Germany.

[2]Department of Chemical Engineering and Bioengineering Program, Lehigh University, Bethlehem, PA 18017, United States.

[3]Department of Chemical Engineering and Department of Science and Technology Unit on Nanoscience, Indian Institute of Technology, Kanpur 208016, India

* Corresponding authors: anj6@lehigh.edu & aghatak@iitk.ac.in

Abstract

We report direct measurement of surface deformation in soft solids due to their surface tension. Gel replicas of PDMS masters with rippled surfaces are found to have amplitudes that decrease with decreasing gel modulus. Surface undulations of a thin elastomeric film are attenuated when it is oxidized by brief exposure to oxygen plasma. Surface deformation in both cases is modelled successfully as driven by surface tension and resisted by elasticity. Our results show that surface tension of soft solids drives significant deformation, and that the latter can be used to determine the former.

1. Introduction

The presence of an interface between two phases results in a change in free energy compared to the bulk [1],[2],[3]; resulting equilibrium properties of an interface are its surface energy, γ, and surface tension, σ. The surface tension is the isotropic part of the surface stress in the surface layer [4]. The surface energy, by contrast, is the work necessary to form unit area of surface by a process of division; surface energy and tension are related by an expression provided by Shuttleworth [5] and subsequently generalized by others [6, 7].

Although surface tension can potentially drive significant deformation in soft solids like hydrogels and elastomers, little attention has been paid to investigating these phenomena or to the problem of measuring surface tension. For example, a neo-natal infant's lungs fail to inflate and collapse unless just the right surfactant is injected. This respiratory distress syndrome (RDS) is governed by surface energy *and* surface tension, and mitigated by their modulation by surfactant adsorption [8]. The ability to create a replica of features in a stiff mold using a soft material is limited by shape rounding or flattening due to surface tension [9]. Adhesion, locomotion, and proliferation of biological cells depends on surface mechanical properties; cells will propagate from the softer to the stiffer portion of a substrate and exert surface stresses which results in surface creases [10]. Importantly, the role of surface tension of the deformed surface on the response of the cell has generally been ignored.

For a liquid, it is well-known that surface tension is positive with a numerical value equal to the surface energy, so that one need not always distinguish between the two. However, it has long been recognized that the surface tension need not equal the surface energy for solids – they need not even have the same sign [5, 11]. In particular, when the two

are different, in Laplace's equation the pressure difference across a curved interface is proportional to the surface tension (*not* the surface energy) times the surface curvature [5, 6]. The deformation caused by this pressure difference for most stiff solids is negligible. However, in highly deformable, soft solids, this need not be the case and surface tension could cause significant deformation.

If a liquid contacts a soft or compliant solid, its surface tension can drive deformation; a characteristic length scale for it is given by the ratio, γ/E, where E is the elastic modulus [9, 12]. While for stiff solids such as metals and ceramics, this is insignificantly small, for soft materials such as elastomers and gels with E in the kPa to MPa range, γ/E ranges from tens of nm to several microns. Such elasto-capillarity phenomena, driven by *liquid surface tension,* have been studied in some detail as reviewed recently [12], but are distinct from phenomena driven by *solid surface tension*.

Deformation of soft solids due to their surface tension has been much less studied. Mora et al. recently showed that a compliant solid cylinder experiences a Rayleigh-Plateau-like instability in which surface tension defines the characteristic length scale [13]. Jerison et al.[14] showed that solid surface tension influences the elastic substrate deformation due to a contact line. Crosby and co-workers [15] have studied bubble growth under pressure in compliant solids, where surface tension plays a significant role. The characteristic length scale in the case of surface tension driven deformation is σ / E. For example, if we attempt to make a sharp edge in a soft elastic solid, this length scale estimates the radius of curvature to which the sharp edge will relax [9]. Adhesive contact between elastic bodies can be used to determine solid-solid interfacial energy [16, 17], but not solid surface tension. The commonly used contact angle measurement, using Young's equation [18], determines not surface tension but differences in surface energy [5, 6].

Gibbs noted [19] that the surface tension is quite a different quantity from surface energy, and the phenomena it drives are generally negligible, because "the rigidity of solids is in general so great, that any tendency of the surfaces of discontinuity to variation in area or form may be neglected in comparison with the forces which are produced in the interior of the solids by any sensible strains…". More recently, de Gennes et al. [1], in a discussion of techniques to measure surface energy or tension of liquids, have noted that, "As such, these methods cannot be readily applied to hard interfaces, whether between a solid and a vapor or between a solid and a liquid, because the elastic energy stored in the solid far exceeds the interface energy associated with any distortion. As a result, measuring the surface tension of solids is generally perceived as an impossible task." While surface stress measurement is difficult, techniques for crystalline materials are available [6, 20-22], although only *changes* in surface stress can be measured accurately.

Here we show that when the material is sufficiently soft, or if a compliant structure is designed, the difficulty pointed out by Gibbs and de Gennes et al. is obviated. We report on two experiments where surface tension drives sufficiently large deformation of a soft solid to make it easily measurable. In contrast to the time-dependent shape evolution of nearly flat interfaces, e.g., as studied by Mullins [23], a significant part of this deformation is nearly instantaneous. This deformation could be used to measure the surface tension.

2. Experimental

PDMS (poly(dimethysiloxane)) sheets with rippled surfaces of different amplitudes ($0.5 - 5\ \mu m$) and wavelengths ($22 - 32\ \mu m$) were fabricated using replica molding as described elsewhere in detail [24] (Figure 1a). Gel replicas of the PDMS rippled surfaces were prepared by pouring on them solutions of Gelatine in water and allowing the latter to

cross-link overnight at a controlled temperature of 7-8 °C inside a refrigerator. In order to vary the elastic modulus of the gel, Gelatine solutions of different concentration were prepared by mixing Gelatine powder (purchased from EWALD-GELATINE GmbH**)** into hot water (60^{o} C) at different weight ratios: 1:10 to 3:10. After gelation, the samples were removed from the refrigerator and allowed to equilibrate to room temperature.

Prior to separation of the gel from the PDMS, we would observe a clear, light-transmitting interface suggesting intimate contact between the two. To confirm more directly that the gel surface matched that of the PDMS faithfully we sectioned a rippled PDMS master normal to the surface and to the ripple direction. The sectioned surface was placed in contact with the bottom of a petri dish after which we poured Gelatine solution, which was allowed to gel following the same procedure as for other samples. The PDMS-Gel sample cross-section was examined by dark-field optical microscopy (Figure 1b). Such micrographs confirmed that the gel faithfully replicated the surface topography of the rippled PDMS. (See also Supplemental Information.[25])

Following this, the gel was gently removed from the PDMS mold. The surface topography of the PDMS master and its gel replica was examined at several spots using a white light interferometer (WLI) (along with MetroPro 8.3.5 software, Zygo Corp. Middlefield, CT USA). Images were analyzed to compute the distributions of successive peak-to-valley heights using code written in Matlab$^{(R)}$. In addition, the dynamics of surface profile evolution was captured by scanning one spot over a period of time until a steady state was attained. Elastic moduli of different gel samples were obtained by indentation using a rigid sphere. The compressive part of the load-displacement curves was analyzed using the Hertz theory of elastic contact [26] to obtain the Young's modulus.

In a separate set of experiements a fibrillar PDMS structure with an undulating terminal film (~ 6-8 μm thick) was fabricated using a process described elsewhere [27] (Figure 1c). We exposed the film briefly (12-30 s) to oxygen plasma (60% O_2, 100% power, Diener electronic GmbH+ Co. KG, Germany). Surface undulations were measured using WLI before and after exposure of the surface to oxygen plasma.

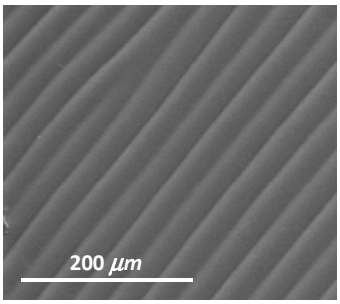

(a)

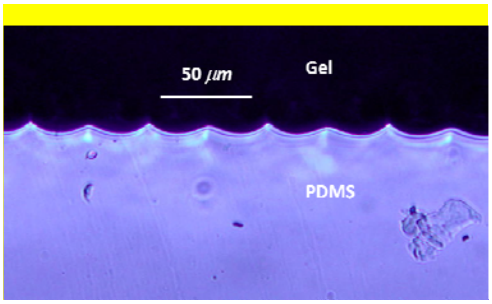

(b)

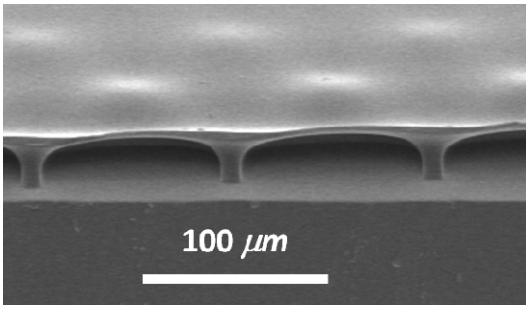

(c)

Figure 1 (a) Scanning electron micrograph of a nearly flat rippled surface, (b) Dark-field optical micrograph: a cross-sectional view of the gel-PDMS interface shows that the gel replicated faithfully undulations in the PDMS surface, and (c) Scanning electron micrograph of a film-terminated structure, both fabricated using an elastomer, PDMS.

3. Flattening of a Gel-Replica by Surface Tension

Figure 2a shows plots of the surface undulations of a PDMS sample (higher amplitude) and its gel replica (smaller amplitude, Young's modulus, E = 18 kPa). Figure 2b shows line scans of the surface profile along paths marked by the lines in Figure 2a. It is evident from these figures that peak-to-valley heights for the gel replica (~0.4 μm) are significantly smaller than those of the PDMS surface against which it was cast (~1.0 μm). Moreover, it appears that sharper features, or higher Fourier modes, are flattened out preferentially in the replica. Figure 2 (c) shows the cumulative distribution of peak-to-valley heights in a different gel sample, again with E = 18 kPa. The mode of the peak-to-valley height distribution of the PDMS master, ~2.7 μm, reduces to ~1.5 μm in the gel replica. The ripple amplitude of the gel replica, following an instantaneous reduction upon separation from its PDMS master, continued to evolve over tens of minutes (Figure 2(d)). Through separate experiments, we confirmed that the fractional volume change due to drying prior to separation of the gel and PDMS is much smaller than the observed fractional change of the surface undulation amplitude (see Supplementary Information for more detail). Therefore, we have focused on the short-time, nearly instantaneous, flattening of the gel surface upon separation from the PDMS master, which is unaffected by gel drying.

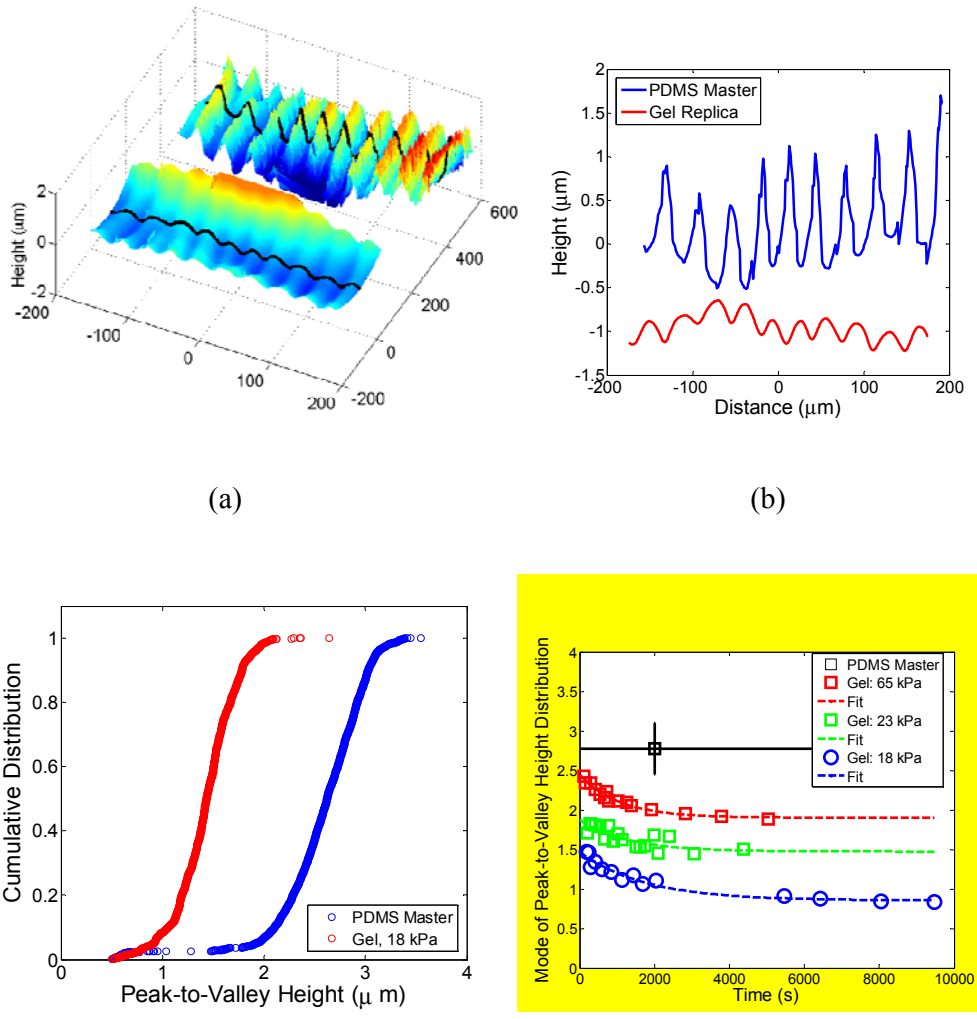

Figure 2 (Color online) (a) Surface plot of ripples on PDMS (higher amplitude) and its gel replica (E = 18 kPa). The in-plane distance is in microns; the average peak-to-peak separation is 31 μm. (b) Line scans of the surface profile for the master PDMS and its gel replica. (The datum is arbitrary.) (c) Cumulative distribution of peak-to-valley heights for a PDMS master and its gel replica (Young's modulus, E = 18 KPa). (d) Evolution of amplitude as a function of time for gels of different moduli.

Figure 3 (a) shows how the short-time mode of the peak-to-valley height distribution of the gel replica decreases systematically with decreasing gel modulus for two different PDMS masters (circles & triangles). The solid lines represent the mean peak-to-valley heights for the PDMS masters.

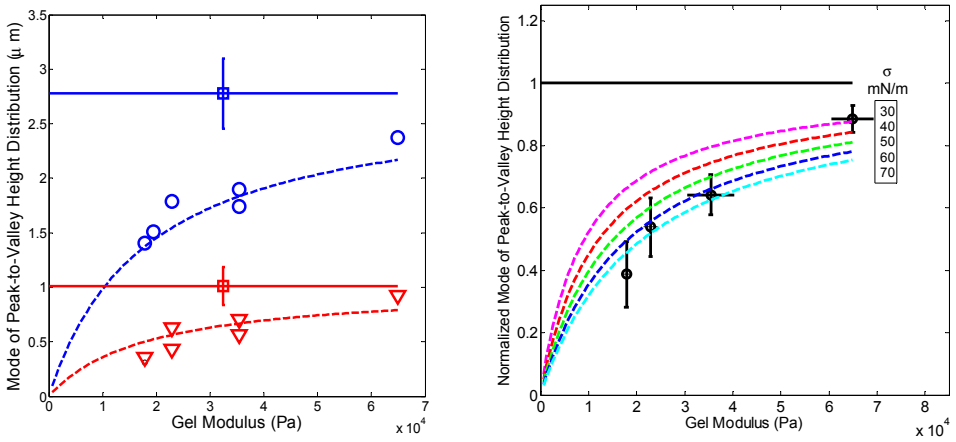

(a) (b)

Figure 3 (Color online) (a) Mode of short-time peak-to-valley height distribution as a function of gel modulus for two different rippled PDMS masters (points). Solid lines represent the PDMS masters; dashed lines are theoretical predictions. (b) Normalized short-time mode of peak-to-valley height distribution as a function of gel modulus. The dashed lines are theoretical predictions using different values of surface tension.

Figures 2 and 3 show that, upon separation from the master PDMS surface, undulations on the gel surface relax significantly. To see whether this shape change can be explained reasonably by surface deformation driven by surface tension, consider the following simple model. Let the surface ripples on the PDMS master be represented by a single sinusoidal function

$$y = a_o \cos\left(\frac{2\pi x}{\lambda}\right) \qquad (1)$$

where a_o is the amplitude and λ is the wavelength. Let a be the amplitude of the gel immediately after it is separated from the master. Because $a/\lambda << 1$, the surface curvature of the gel can be estimated accurately by y'', the second derivative. Laplace's equation for pressure difference across a curved surface, p, gives

$$p = -a\sigma\left(\frac{4\pi^2}{\lambda^2}\right)\cos\frac{2\pi x}{\lambda} \tag{2}$$

Assuming a constant surface tension, the resulting displacement of the surface due to this pressure is given by [26]

$$u = -4\pi\left(\frac{a}{\lambda}\right)\left(\frac{\sigma}{E*}\right)\cos\frac{2\pi x}{\lambda} \tag{3}$$

where $E*$ is the plane strain modulus. Thus, the rippled gel surface has a *reduced* amplitude of

$$a = \frac{a_o}{1+4\pi\left(\frac{\sigma}{E*\lambda}\right)} \approx a_o\left(1-4\pi\left(\frac{\sigma}{E*\lambda}\right)\right); \tag{4}$$

where the approximate version in eq. (4) holds if the change in amplitude is small compared to the amplitude itself. For such small changes in amplitude, by superposition, we can consider more general surfaces. Specifically, if $a^i{}_o$ is the coefficient of the 'ith' Fourier mode on the master, it is reduced in the replica to

$$a^i = a^i{}_o\left(1-4\pi\left(\frac{\sigma i}{E*\lambda}\right)\right); \tag{5}$$

That is, higher modes are proportionately attenuated to a greater extent by surface tension, as is evident qualitatively in Figure 2b.

A hydrogel surface essentially comprises mostly water, bound to the cross-linked protein network. Accordingly, we expect the surface tension, σ, to be on the order of the surface energy of water, and somewhat smaller in magnitude. The dashed lines in Figure 3(a) show the predicted peak-to-valley height (twice the amplitude) given by eq. (4) using a value

of 60 mN/m for surface tension. Figure 3(b) shows data from a few different samples and plots a/a_o as a function of Young's modulus. The solid lines are calculated using eq. (4), for surface tension values ranging from 30-70 mN/m. We may expect that as modulus reduces and the fraction of water in the hydrogel increases, the surface tension would increase and approach the value of pure water. Therefore, potentially, the procedure followed above could be run in reverse, and measured deformation be used to estimate an (unknown), composition-dependent, surface tension.

4. Surface Undulations of a Thin PDMS Plate

The interplay between surface tension and elasticity is further examined in a different experiment in which we compare surface undulations of a film-terminated fibrillar PDMS sample before and after exposure to oxygen plasma, Figures 4 (a) and (b). Taking peaks as the datum, Figure 4(c) plots final peak-to-valley heights for a number of points in a sample with fibril separation of 110 μm. The surface has well-defined periodic undulations that are evidently reduced systematically following exposure to the oxygen plasma.

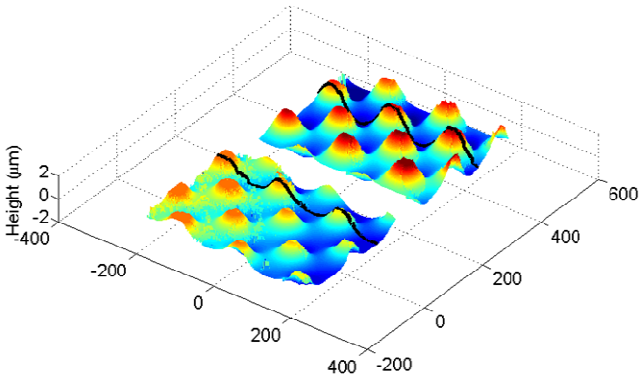

(a)

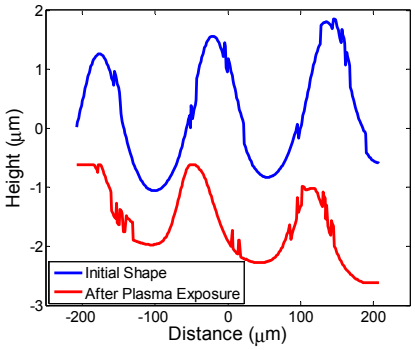

(b)

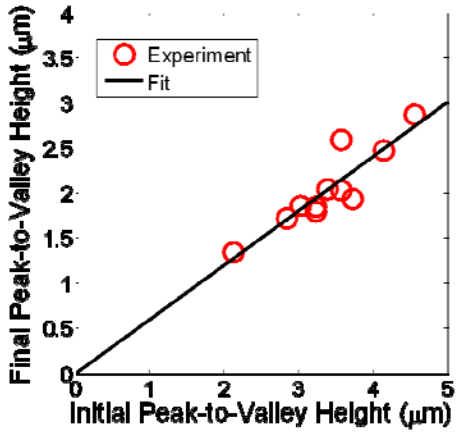

(c)

Figure 4 (Color online) (a) Surface plot of height undulations in the PDMS film before (higher amplitudes) and after (lower amplitudes) exposure to oxygen plasma, (b) Line scan across the surface shows that exposure to oxygen plasma flattens the surface, (c) Final peak-to-valley heights are systematically lower than their initial values.

As fabricated, the terminal film (Figure 1c) lies on a silicon wafer and has a flat surface; this is its stress-free configuration. However, the inner surface of the terminal film is not flat; let this shape be $w_o(x.y)$. When the sample is separated from the flat silicon wafer on which it is fabricated, the film is released from its constraint, and the action of surface tension on the interior surface causes the film to deform to a shape given by $w_f(x.y)$ (Figures 1(c), 4(b)).

Curvature of the upper and lower surfaces multiplied by surface tension is the Laplace pressure which drives deformation. The following equation governs deformation of a plate subjected to surface tension ([28], see also Supplemental Information)

$$D\nabla^4 w_f = \sigma\nabla^2(w_o); \tag{6}$$

where $D=E^*t^3/12$ is the flexural rigidity, and t is the film thickness. The non-uniformity of the plate thickness, and the fact that the plate is constrained by posts, make an exact analysis cumbersome. We opt instead for an approximate model that provides a scaling result by choosing to represent shape and deformation as:

$$\begin{aligned} w_o &= c_o\left(2-\cos\left(\frac{2\pi x}{b}\right)-\cos\left(\frac{2\pi y}{b}\right)\right) \\ w_f &= c_f\left(2-\cos\left(\frac{2\pi x}{b}\right)-\cos\left(\frac{2\pi y}{b}\right)\right) \end{aligned}; \tag{7}$$

(See Figure S3 in Supplemental Information.) Substituting (7) into (6) provides the result

$$c_f = -c_o\frac{\sigma b^2}{4\pi^2 D} = -\frac{\sigma}{E^*}\frac{3c_o b^2}{\pi^2 t^3} \tag{8}$$

Note that the characteristic length scale σ/E^* is amplified by a geometric factor, $3c_o b^3/\pi t^3 >> 1$. Based on measured values of c_f (Figure 4b), PDMS modulus (4 MPa [29]), and thickness (~7 μm), this equation is consistent with known surface energy of PDMS (22 mN/m [30]) for c_o ~ 6-7 μm, a reasonable value (Figure 1c). It is known that plasma treatment creates a thin silicaceous surface film [31]. For the short exposures such as used in this work, it is expected to be ~ 6 nm in thickness with a Young's modulus of 1.5 GPa modulus [29]. The bending rigidity of the PDMS film changes from $D = E^* t^3/12$ approximately to $D = E^* t^3/12 + E_s^* t^2 t_s/4$, where t_s, E_s*, are the thickness and Young's modulus of the silica film. Then, according to equation (8), the amplitude of undulations

should reduce by the ratio of bending rigidity. Using the same parameters as cited above, we calculate this reduction to be a factor of 0.56, consistent with measurements (Figure 4c).

5. Concluding Remarks

In summary, we have shown that soft elastic solids have a surface tension that can drive significant deformation. For a rippled surface, the amplitude change of the replica is governed by the characteristic length scale, σ / E, attenuated by the ripple geometrical factor, $a_o / \lambda < 1$. For the thin-plate geometry, the characteristic length scale, amplified by the plate geometrical factor, $c_o b^2 / t^3 >> 1$, approximates the observed changes in surface undulations. With an appropriate choice of geometry, deformation can thus be used to measure the surface tension of soft solids over a range of elastic moduli.

6. Acknowledgements

AJ's contribution was supported in part by the U.S. Department of Energy, Office of Basic Energy Sciences, Division of Materials Sciences and Engineering under award DEFG02-07ER46463. AJ also gratefully acknowledges the support of the Leibniz Institute for New Materials in Saarbruecken during his sabbatical leave. AG acknowledges support from the Humboldt Foundation in the form of a fellowship for this work. All authors would like to acknowledge the support of and discussions with Prof. E. Arzt of the Leibniz Institute for New Materials in Saarbruecken. The PDMS masters were fabricated by Dr. K. Khare in the laboratory of Prof. Shu Yang, to both of whom we are grateful for providing those samples. We thank Ms. Nichole Nadermann for preparing the film-terminated samples and Figure 1c. We thank Ms. Jinkyung Pyo for help with preparation of gelatine samples. The authors would also like to acknowledge many useful discussions with Prof. Manoj Chaudhury.

7. References

1. deGennes, P.-G., F. Brochard-Wyart, and D. Quere, *Capillarity and Wetting Phenomena. Drops, Bubbles, Pearls, Waves*. 2002, New York: Springer Science+Business Media, Inc.
2. Rowlinson, J.S. and B. Widom, *Molecular Theory Of Capillarity*. 1989, New York, USA: Oxford University Press.
3. Adamson, A.W. and A.P. Gast, *Physical Chemistry of Surfaces*. 1997, New York: John Wiley & Sons.
4. *In the systems studied in this work, the surface is isotropic, i.e., the surface stress is represented by a single number, the surface tension (formally half of the trace of the surface stress, following Shuttleworth [5]).*
5. Shuttleworth, R., *The Surface Tension of Solids.* Proceedings of the Physical Society. A, 1950. 63(5): p. 444.
6. Robert C. Cammarata, K.S., *Surface and Interface Stresses.* Annual Review of Materials Science, 1994. 24: p. 214-234.
7. Herring, C., *The Use of Classical Macroscopic Concepts in Surface-Energy Problems*, in *Structure and Properties of Solid Surfaces*, R. Gomer and C.S. Smith, Editors. 1953, The University of Chicago Press: Chicago. p. 5-71.
8. Chida, S., et al., *Surfactant proteins and stable microbubbles in tracheal aspirates of infants with respiratory distress syndrome: relation to the degree of respiratory failure and response to exogenous surfactant.* Eur. J. Pediatr., 1997. 156: p. 131-138.
9. Hui, C.-Y., et al., *Constraints on Micro-Contact Printing Imposed by Stamp Deformation", .* Langmuir, 2002. 18: p. 1394-1404.
10. Burton, K. and D.L. Taylor, *Traction forces of cytokinesis measured with optically modified elastic substrata.* Nature, 1997. 385: p. 450-454.
11. Orowan, E., *Surface Energy and Surface Tension in Solids and Liquids.* Proceedings of the Royal Society, London, A, 1970. 316(1527): p. 473-491.
12. Roman, B. and J. Bico, *Elasto-capillarity: deforming an elastic structure with a liquid droplet.* Journal of Physics: Condensed Matter, 2010. 22(49).
13. Mora, S., et al., *Capillarity Driven Instability of a Soft Solid.* Physical Review Letters, 2010. 105 p. 214301.
14. Jerison, E.R., et al., *Deformation of an Elastic Substrate by a Three-Phase Contact Line.* Physical Review Letters, 2011. 106(18): p. 186103.
15. Jessica A. Zimberlin, N.S.-D., Gregory N. Tew, Alfred J. Crosby, *Cavitation rheology for soft materials.* Soft Matter, 2007. 3: p. 763-767.
16. Chaudhury, M.K. and G.M. Whitesides, *Direct measurement of interfacial interactions between semispherical lenses and flat sheets of poly (dimethylsiloxane) and their chemical derivatives.* Langmuir, 1991. 7(5): p. 1013-1025.
17. Haidara, H., M.K. Chaudhury, and M.J. Owen, *A direct method of studying adsorption of a surfactant at solid-liquid interfaces.* The Journal of Physical Chemistry, 1995. 99: p. 8681-8683.
18. Chaudhury, M.K., *Interfacial interaction between low-energy surfaces.* Materials Science and Engineering Reports, 1996. 16: p. 97-159.
19. Gibbs, J.W., *Collected Works 1 p315*. 1876, London: Longman and Green.
20. Sander, D., *Surface stress: implications and measurements.* Current Opinion in Solid State and Materials Science, 2003. 7: p. 51-57.
21. Nicolson, M.M., *Surface Tension in Ionic Crystals.* Proceedings OF THE ROYAL SOCIETY A-MATHEMATICAL PHYSICAL AND ENGINEERING SCIENCES, 1955. 228(1175): p. 490-510.
22. Berger, R., et al., *Surface Stress in the Self-Assembly of Alkanethiols on Gold.* Science, 1997. 276: p. 2021-2024.

23. **Mullins, W.W., *Flattening of a Nearly Plane Solid Surface due to Capillarity.* Journal of Applied Physics, 1959. 30(1): p. 77-83.**
24. **Vajpayee, S., et al., *Adhesion Selectivity Using Rippled Surfaces.* Advanced Functional Materials, 2011. 21: p. 547-555.**
25. ***Supplemental Material contains (1) a discussion showing that the flattening of the gel surface conserves volume, (2) that the gel replicates faithfully the rippled PDMS master prior to separation of the two, (3) discussion of time-dependent evolution of the surface profile of the gel, and (4) some details on the analysis of flattening of the film-terminated surface.***
26. **Johnson, K.L., *Contact Mechanics*. 1985, Cambridge: Cambridge University Press.**
27. **Nadermann, N., et al., *Active Switching of Adhesion in a Film-Terminated Fibrillar Structure.* Langmuir, 2010. 26(19): p. 15464–15471.**
28. **Timoshenko, S. and S. Woinowsky-Krieger, *Theory of plates and shells*. 1959: McGraw-Hill.**
29. **Noderer, W.L., et al., *Enhanced adhesion and compliance of film-terminated fibrillar surfaces.* Proceedings of the Royal Society a-Mathematical Physical and Engineering Sciences, 2007. 463(2086): p. 2631-2654.**
30. **She, H., D. Malotky, and M.K. Chaudhury., *Estimation of Adhesion Hysteresis at Polymer/Oxide Interfaces Using Rolling Contact Mechanics.* Langmuir, 1998. 14(11): p. 3090–3100.**
31. **Béfahy, S.p., et al., *Thickness and Elastic Modulus of Plasma Treated PDMS Silica-like Surface Layer.* Langmuir, 2010. 26(5): p. 3372.**